An ultra-sensitive optical MEMS sensor for partial discharge detection

An ultra-sensitive optical MEMS sensor for partial discharge detection

Xiaodong Wang[1]**, Baoqing Li**[1]**, Zhixiong Xiao**[1]**, Sang Hwui Lee**[1]**, Harry Roman**[2]**, Onofrio L Russo**[1]**, Ken K Chin**[1] **and Kenneth R Farmer**[1]

[1] Department of Physics, New Jersey Institute of Technology, Newark, NJ 07102, USA
[2] PSE&G Company (T-10A), 80 Park Plaza, PO Box 570, Newark, NJ 07102, USA

E-mail: xw3@njit.edu

Abstract

A diaphragm-based interferometric fiber optical microelectromechanical system sensor with high sensitivity is designed and tested for on-line detection of the acoustic waves generated by partial discharges (PD) inside high-voltage power transformers. In principle, the sensor is made according to Fabry Perot interference, which is placed on a micro-machined rectangular silicon membrane as a pressure-sensitive element. A fiber-optic readout scheme has been used to monitor sensor membrane deflection. Sensor design, fabrication, characterization, and application in PD acoustic detection are described. Test results indicate that the fiber optical sensor is capable of detecting PD acoustic signals propagating inside transformer oil with high sensitivity.

(Some figures in this article are in colour only in the electronic version)

1. Introduction

This paper describes the work that develops a fiber optical sensor system for partial discharge (PD) acoustic detection. PD occurring under oil produces an acoustic pressure wave that is transmitted throughout the transformer via the oil medium [1–5]. One can achieve PD acoustic detection by mounting piezoelectric acoustic sensors externally on the walls of the power transformer. An externally mounted piezoelectric acoustic sensor offers the advantages of easy installation and replacement. However, a piezoelectric sensor may suffer from degeneration of the signal-to-noise ratio caused by environmental noises such as electromagnetic interference (EMI). Another disadvantage associated with the externally mounted piezoelectric sensor is that the multiple paths of acoustic wave transmission make locating the exact positions of PD difficult. It is thus desirable to have sensors that can function reliably inside a transformer to accurately locate PD-induced acoustic signals. For the sake of safety and easy installation, these sensors have to be chemically inert, electrically nonconducting, passive and small in size. Optical fiber-based sensors have been shown to be attractive devices which measure a wide range of

physical and chemical parameters, because the sensors have a number of inherent advantages, including small size, light weight, high sensitivity and immunity to EMI noise. These advantages make optical fiber sensors excellent candidates for PD acoustic detection. Optically interrogated pressure sensors have been demonstrated in various configurations using microelectromechanical system (MEMS) technology [6–12], but sensitivities of these devices are low for PD acoustic signal detection. In this paper, we describe an ultra-sensitive optical sensor for PD acoustic detection.

2. Sensor operation principle and design

Figure 1 shows the schematic of the whole fiber optical sensor system. The system consists of a sensor probe, a 1310 nm LED, a 3 dB fiber optic coupler, a low noise optical receiver (photodiode), and single-mode fibers linking the sensor and the optical receiver. In the system, a laser source (1310 nm) is used as the light source, and an optical signal is converted to an electrical signal by the photodiode. The light is launched into the sensor through the coupler. The light reflected from the sensor is transmitted back through the coupler to the photodiode.
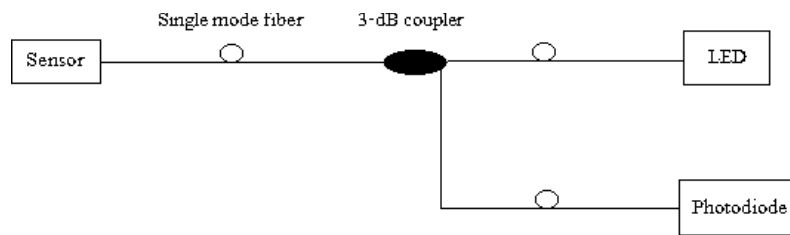
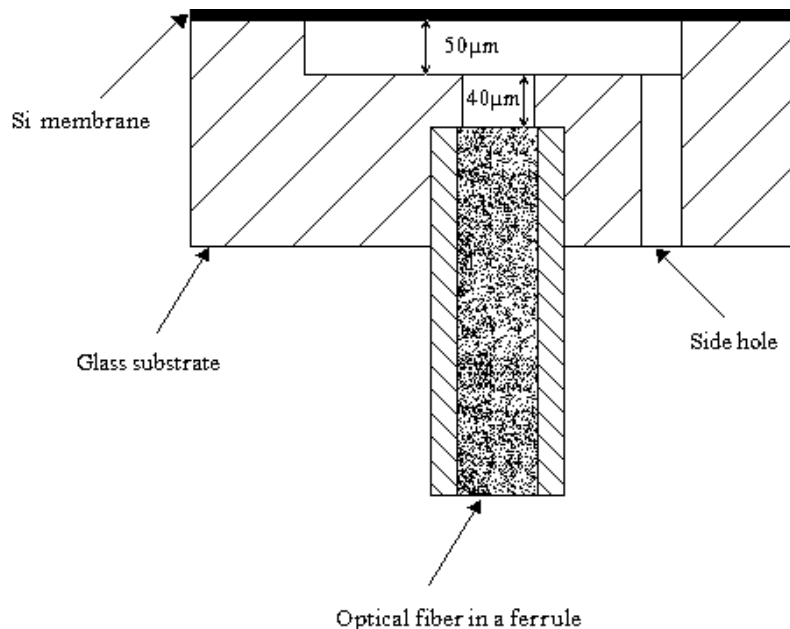**Figure 1.** Operation principle of the fiber optical sensor.

Figure 2. Sensor head design.

The sensor described in this paper has just one fiber. It consists of a Fabry Perot interferometer integrated into a single-mode optical fiber. This interferometer converts the phase changes into variations of the reflected and transmitted optical power. The optical sensor is illustrated schematically in figure 2. The incident light is first partially reflected (R_1) at the end face of the fiber. The remainder of the light propagates across an air gap to the inner surface of the membrane, where it is once again partially reflected (R_2). The multiple reflections travel back along the same fiber and through the fiber coupler to the optical receiver. The received optical intensity I_r can be expressed by [13]

$$I_r = I_0 \frac{R_1 + R_2 - 2\sqrt{R_2 R_1} \cos(\phi)}{1 + R_2 R_1 - 2\sqrt{R_2 R_1} \cos(\phi)} \qquad (1)$$

where I_0 is the laser source power; ϕ is the round trip phase shift of the light inside the air gap given by

$$\phi = \frac{4\pi n L}{\lambda} \qquad (2)$$

where L is the length of the air gap, $n = 1$ the refractive index of the air, and λ the wavelength of the light source.

The PD acoustic signal causes deflection of the membrane and modulates the air-gap length. The sensor therefore yields outputs that correspond to the applied acoustic signals. The output signal from the sensor system should be a periodic function of changes in the gap length. Summarizing, although the circuit provides time-series data, the output is a spatially
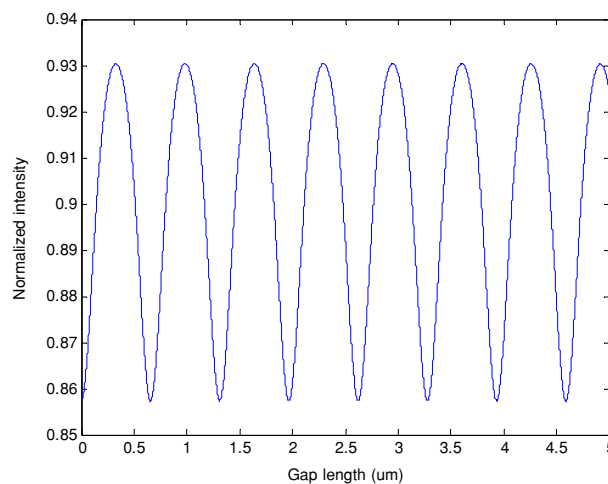

Figure 3. The relationship between normalized intensity and gap length.

varying function of changes in the sensor gap length. It is useful to plot the detected intensity versus gap length L, as shown in figure 3. According to figure 3, a fringe period corresponds to an air-gap change of one half of the optical wavelength, which in our case is 655 nm. Figure 4 shows that the normalized intensity increases with increased reflectance.

If the pressure is applied to the membrane and causes the gap length changes by ΔL (membrane center deflection), the
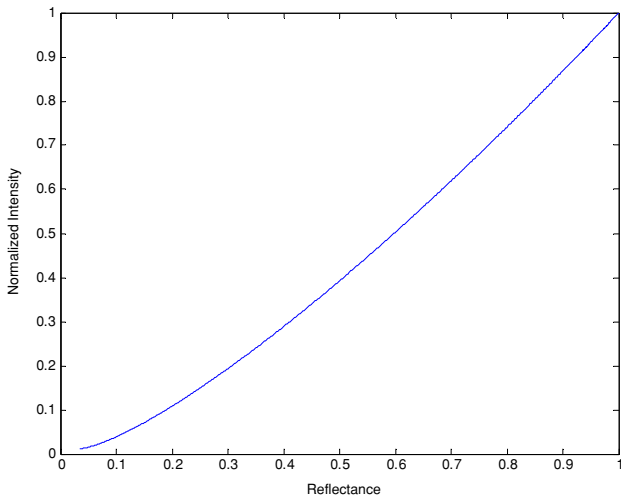
Figure 4. The relationship between normalized intensity and reflectance.

round trip optical phase change will be $\Delta\phi = 4\pi n\Delta L/\lambda$. With the assumption of uniform membrane thickness, small deflections (deflection less than 25% of the membrane thickness), infinitely rigid clamping about the periphery of the square membrane, and perfectly elastic behavior, which is almost true for the silicon membrane and our bonding method, the linear relationship between a flat square membrane center deflection and pressure difference P can be expressed as [14]

$$\Delta L = \frac{Pa^4(1-v^2)}{4.2Eh^3} \qquad (3)$$

where P is the ambient pressure related to the cavity pressure (Pascal), ΔL the center deflection of the membrane, a the half side length, h the membrane thickness, E the Young modulus, and v is the Poisson ratio of the membrane material.

The thickness and side length of the membrane are selected depending upon the pressure range within which the device is required to operate. Due to high sensitivity requirement for PD acoustic detection, silicon membrane with a thickness of 25 μm and a side length of 2 mm is selected. ANSYS simulation shows that the natural frequency of the membrane is around 91 kHz (figure 5).

3. Fabrication of the sensor

The fiber optical sensor (as shown in figure 2), consisting of a thin silicon membrane and a micromachined substrate (500 μm thick Pyrex 740 glass wafer) with a cavity and a hole for the fiber, is fabricated in a clean room in one step: anodic wafer bonding using the EV501 bonder. In order to increase the reflectance, about 100 Å of gold is evaporated on the silicon membrane. The wafer is then diced and individual sensors are separated for packaging.

The depth of the square cavity is 50 μm. A center hole in the glass substrate is used to place a ferruled fiber for Fabry Perot interrogation. The cavity between the fiber end and glass surface is 105 μm wide and 40 μm deep. The width of the cavity is smaller than the fiber diameter so that the cavity serves as a stop for the fiber and sets the baseline depth of the fiber. The final chip size is about 3×3 mm^2. The total chip thickness is around 530 μm.

With the sensor inserted inside the transformer, a static oil pressure that can be as high as 8 psi will make the membrane work in a nonlinear region. An additional hole with the diameter of 400 μm drilled through the glass wafer into the cavity allows pressure measurements to be related to the surrounding pressure.

A stainless steel housing for the sensor that has been designed and fabricated has the sensor placed at one end as shown in figure 6. A 7 inch long tube is also attached to a drain plug by a compression fitting. The end of the housing opposite to the sensor contains a stainless steel tee fitting. One fitting
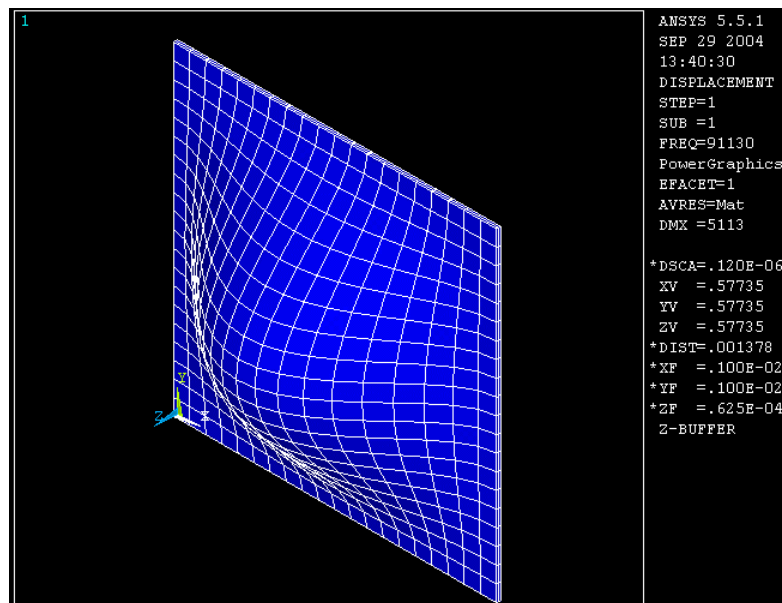

Figure 5. ANSYS simulation of the silicon membrane.

Figure 6. A packaged sensor.

of the tee is for the optical fiber and the other is to control the sensor backside pressure and environment.

4. Sensor testing

Our sensor testing includes three parts: sensitivity, frequency response and resolution.

4.1. Sensitivity

The sensor sensitivity experimental setup is shown in figure 7. As a reference sensor that gives information about the applied pressure, a Motorola sensor (MPXV5004GC6U) has a linear output (1–5 V) when the pressure changes from 0 to 4 kPa. Since the sensor system noise is 100 mV, the smallest pressure that the Motorola sensor can measure is 100 Pa. The fiber optical and Motorola sensors are connected to the same pressure source using a T-connector. The tube fittings make a good nonleakage connection between the T-connector and the plastic pipe. Super glue is used in the connection between the sensors and plastic pipes. The outputs of the sensors are sent to a data logger and then to the computer for analysis.

The sensitivity measurements begin by opening valve 1 slightly, and then we use the valve 2 to adjust the pressure until pressure regulator 2 reads around 0.6 psi (around 4 kPa). Then making sure that the pressure cap of the T-connector 1 is attached, insure that air pressure can flow to the two sensors. Moreover when we disconnect the pressure cap, the air pressure will be released from T-connector 1 and the
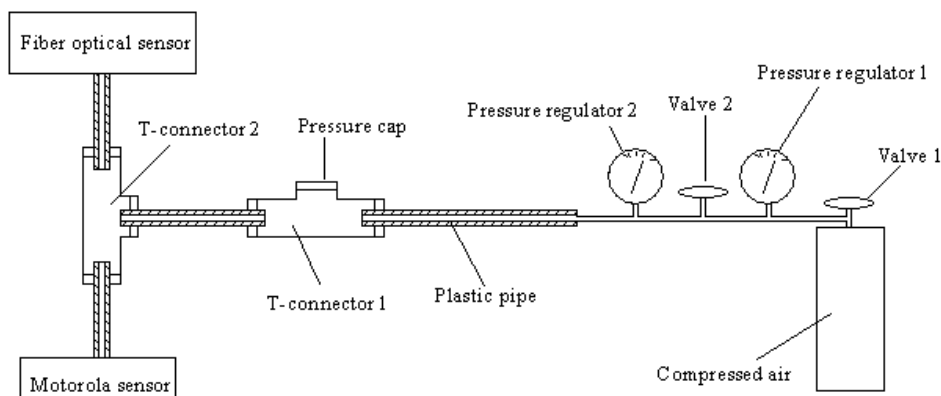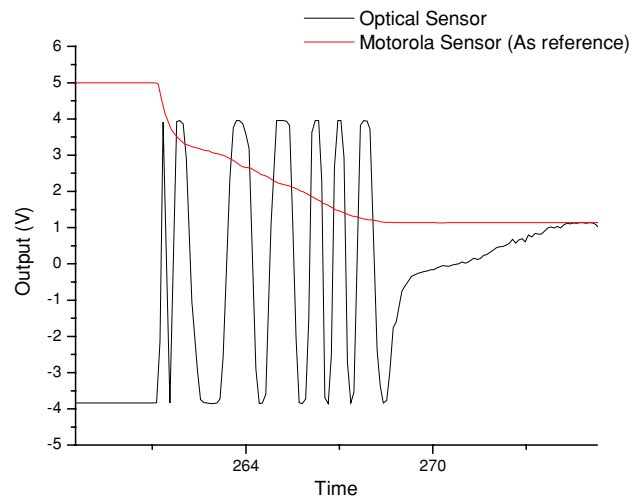

Figure 8. Optical and Motorola sensors' measurement results.

pressure will drop from 4 kPa to 0. Figure 8 shows the outputs of two sensors when the pressure drops from 4 kPa to 0. According to figure 8, when the pressure decreases from 4 kPa to 0, the output of the Motorola sensor decreases linearly from 5 V to 1 V and the optical sensor has about 7.25 periods over same pressure range. This means that about 552 Pa will give a fringe period. Since the pressure change is not linear with time, fringe spacings result in different periods as a function of time. Since each fringe period indicates that the gap length has changed by half of the laser wavelength, 7.25 fringes indicate that the membrane deflection is 4.748 μm. Considering the membrane thickness of 25 μm and a small deflection (deflection less than 25% of the membrane thickness) of 4.748 μm, the membrane deflection is linear with respect to the applied pressure.

4.2. Frequency response

In the experiment, the optical sensor is used to measure the acoustic signal with a single frequency (1 kHz, 2 kHz, up to 100 kHz) generated by a function generator. The sensor output is sent to a dynamic signal analyzer (Standford research system model SR785) for spectrum measurements. For these measurements, we use the dynamic signal analyzer (the
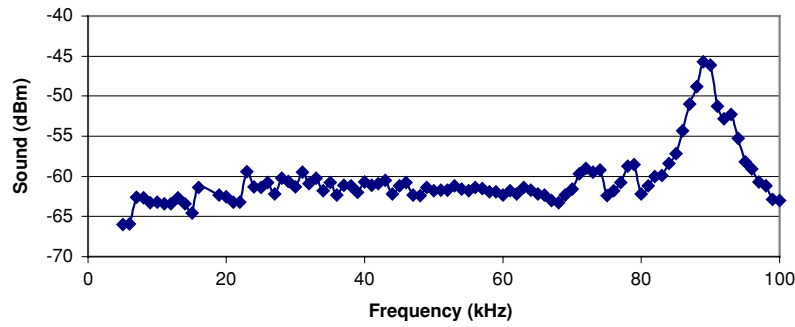

Figure 7. Sensor sensitivity measurement setup.

Figure 9. Frequency response of the fiber optical sensor.

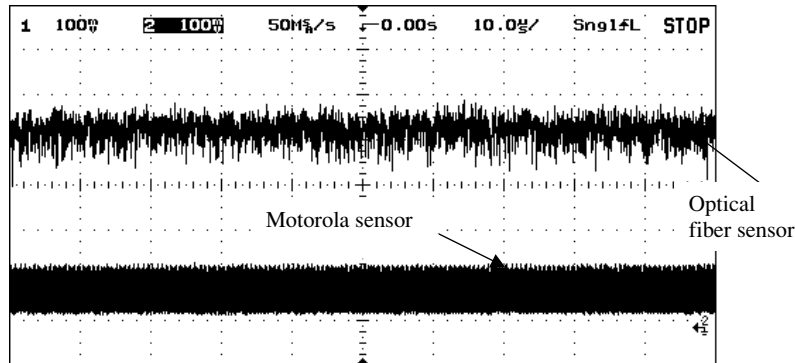**Figure 10.** Noise levels of the fiber optical and Motorola sensors.
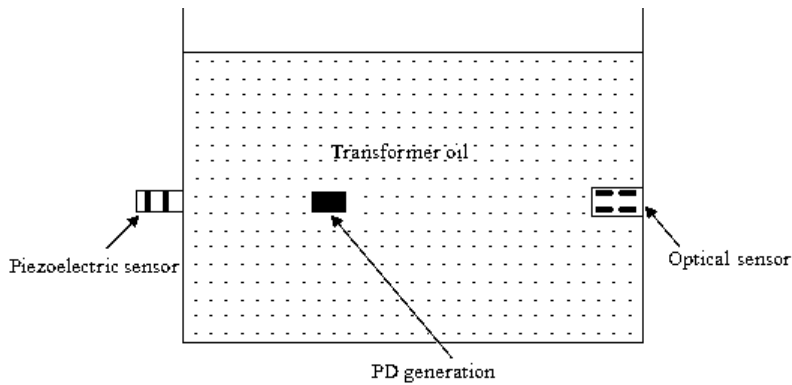

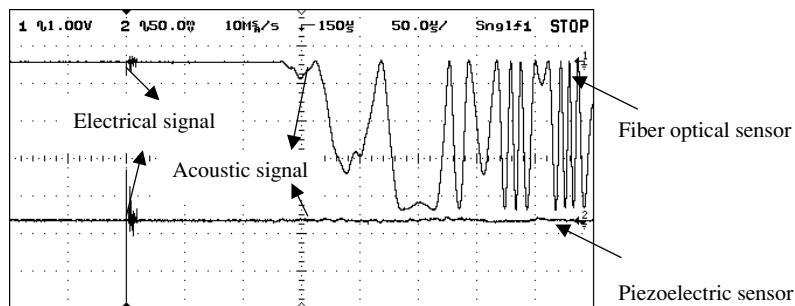**Figure 11.** PD detection experiment setup.

Figure 12. PD detection using the piezoelectric and fiber optical sensors at same distance from the source.

input impendence of 1 MΩ) to select the desired frequency to make the required spectrum (power versus frequency). The resulting measurement scans show received power in the desired frequency, and in decibels relative to mW (dBm).

Figure 9 shows the sensor response to acoustic signals with same amplitude and increasing frequencies, up to 100 kHz. For this measurement, the membrane has an expected resonant frequency of ∼90 kHz. The sensor is seen to have a fairly broad resonance centered on ∼90 kHz, with
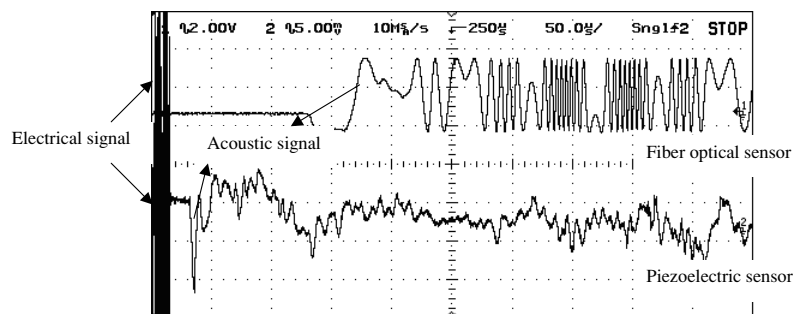
Figure 13. PD detection using the piezoelectric and fiber optical sensors at different distances from the source.

small structure peaks below this frequency. It shows that the sensor has a dynamic response that is close to the expected value.

4.3. Resolution

The pressure measurement resolution of a sensor is limited by the signal-to-noise ratio of the sensor. According to figure 10, the output of the optical fiber sensor noise is around 100 mV. The output of the sensor is from −4 to 4 V corresponding to a half of a period. Since one period corresponds to 552 Pa of applied pressure, the pressure measurement resolution of a sensor is around 2.8 Pa.

5. Sensor's application in PD detection

We set up an experimental system to evaluate optical sensor performance in PD acoustic detection. The standard acoustic methods used to detect PD employ piezoelectric external sensors. As shown in figure 11, the fiber optical sensor is installed in transformer oil at one end of the tank, facing a piezoelectric acoustic sensor (Harisonic G-0504 type) at the other end of the tank. The piezoelectric sensor has an acoustic frequency response up to 5 MHz. The PD generation system (also called PD source) is inside the tank. This arrangement is chosen because it represents many practical PD test situations in which piezoelectric sensors are attached to the sidewall of a transformer, whereas fiber optical sensors can be inserted into the transformer tank. A two-channel digital oscilloscope (HP Model 54616C) is used to display and store the acoustic signals caught by two sensors. The experimental results for the two sensors are shown in figure 12 when they are placed at the same distance (0.4 m) from the PD source. The piezoelectric sensor almost shows no response to the acoustic signals even when the output unit is set as 50 mV, compared to the unit 1 V for the optical sensor which clearly captures the signals.

Since the PD manifests itself as an electrical and acoustic signal, figure 12 shows that both the optical and piezoelectric sensors pick up the electrical signals almost at the same time. This is because the speed of the electrical wave is much faster than acoustic speed. It is similar to lightning and thunder. Because the electrical signal is picked up by the steel housing containing the optical sensor, it is shown in figure 3. However, as shown in figure 13, the optical signal is unaffected by the electrical signal. This is a prototype model and the housing can be changed to some material that is not affected by electrical signals.

Since the piezoelectric sensor cannot detect the signals when it is 0.4 m from the PD source, the piezoelectric sensor is mounted inside the tank and much closer to the source, while the optical fiber sensor is still 0.4 m from the source. The measurement results are shown in figure 13 (output voltage unit for the optical sensor is 2 V and for the piezoelectric sensor 5 mV). As the piezoelectric sensor is much closer to the PD source than the optical sensor, and due to the constant sound velocity in the transformer oil (around 1500 m s^{-1} [15]), the acoustic signal arrives at the piezoelectric sensor earlier than at the optical sensor. But the detected signal is still very weak compared to the optical sensor. These experiments show the sensitivity of the piezoelectric sensor is not as good as the optical sensor for the PD acoustic detection.

6. Conclusions

An optical fiber sensor with ultra-sensitivity is designed, fabricated, and tested. The experiments have shown that the sensitivity of the sensor is enough for PD acoustic detection. The optical sensor offers additional advantages in extremely harsh environments (high temperature, EM interference, dust, etc) in which electronics is not viable. A simple micromachining process compatible with MEMS has been developed for fabricating the optical fiber sensor. The use of MEMS technology is advantageous because of the potential for enormous economical manufacturing.

References

[1] Harrold R T 1985 Acoustical technology applications in electrical insulation and dielectrics *IEEE Trans. Electr. Insul.* **20** 3–19
[2] Unsworth J and Unsworth J 1994 On-line partial discharge monitor for high voltage power transformers *Proc. 4th Int. Conf. on Properties and Applications of Dielectrics Materials Brisbane Australia, 3–8 July*
[3] Varlow B R, Auckland D W and Smith C D 1999 Acoustic emission analysis of high voltage insulation *IEE Proc. Sci. Meas. Technol.* **146** 260–3

[4] Sakoda T 1999 Analysis of acoustic emissions caused by the partial discharge in the insulation oil *Proc. 13th Int. Conf. on Dielectric Liquids (Japan, July 1999)* pp 483–6

[5] Deheng Z 1988 The study of acoustic emission method for detection of partial discharges in power transformers *IEEE Trans. Electr. Insul.* **2** 614–7

[6] Kim Y and Neikirk D P 1995 Micromachined Fabry-Pérot cavity pressure transducer *IEEE Photonics Technol. Lett.* **7** 1471–3

[7] Han J and Neikirk D P 1996 Deflection behavior of Fabry-Perot pressure sensors having planar and corrugated membrane *SPIE's Micromachining and Microfabrication '96 Symposium: Micromachined Devices and Components II: Proc. SPIE 2882 (Austin, USA, 14–15 Oct.)* ed R Roop and K Chau pp 79–90

[8] Gander M J, MacPherson W N, J D C , Stevens R, Chana K S, Anderson S J and Jones T V 2003 Embedded micromachined fiber-optic Fabry-Perot pressure sensors in aerodynamics applications *Sensors J. IEEE* **3** 102–7

[9] Pinnock R A 1998 Optical pressure and temperature sensors for aerospace applications *Sensor Rev.* **18** 32–8

[10] Angelidis D and Parsons P 1992 Optical micromachined pressure sensor for aerospace applications *Opt. Eng.* **31** 1638–41

[11] Beggans M H, Ivanov D I, Fu S G, Digges T G Jr and Farmer K R 1999 Optical pressure sensor head fabrication using ultra-thin silicon wafer anodic bonding *Proc. SPIE—Int. Soc. Opt. Eng.* **3680** 773–82

[12] Mendez A, Morse T F and Ramsey K A 1993 Micromachined Fabry-Pérot interferometer with corrugated silicon membrane for fiber optic sensing applications *Proc. SPIE—Int. Soc. Opt. Eng.* **1793** 170–82

[13] Heavens O S 1955 *Optical Properties of Thin Solid Films* (London: Butterworths Scientific Publications) pp 56–9

[14] Di Giovanni M 1982 *Flat and Corrugated Membrane Design Handbook* (New York: Mercel Dekker)

[15] Sakoda T 1999 Analysis of acoustic emissions caused by the partial discharge in the insulation oil *Proc. 13th Int. Conf. on Dielectric Liquids (Japan, July 1999)* pp 483–6